International Journal of Control, Automation and Systems 19(1) (2021) 29-39
http://dx.doi.org/10.1007/s12555-019-0904-9
ISSN:1598-6446 eISSN:2005-4092
http://www.springer.com/12555

Virtual Model Reduction-based Control Strategy of Planar Three-link Underactuated Manipulator with Middle Passive Joint

Zixin Huang, Xuzhi Lai*, Pan Zhang, Yawu Wang, and Min Wu

Abstract: This paper presents a position control strategy for a planar active-passive-active (APA) underactuated manipulator with second-order nonholonomic characteristics. According to the structural characteristics of the planar APA system, we divide the system into two parts: a planar virtual Pendubot (PVP) and a planar virtual Acrobot (PVA). For the PVP, we mainly fulfill the target angle of the first link, which is calculated through the geometry method, and make the system stable. In this stage, via keeping the states of the third link being zero, the system is reduced to the PVP. Meanwhile, we design an open-loop control law based on the nilpotent approximation (NA) model of the PVP to make the second link stable and the first link stabilize at its target angle. Then, the planar APA system is reduced to a PVA with all links' angular velocities being zero. For the PVA, we mainly realize the other two links' target angles obtained via the particle swarm optimization (PSO) algorithm. Thus, the control objective of the planar APA system is achieved. Finally, above control strategy is verified by simulation results.

Keywords: Nilpotent approximation, planar underactuated manipulator, position control, PSO algorithm, second-order nonholonomic characteristics.

1. INTRODUCTION

For an underactuated system (US), its control inputs are less than the degrees of freedom [1–4]. Apparently, because of the reduction of control inputs, control of such system is difficult. A typical representative of the US is a planar underactuated manipulator (UM) [5, 6] without gravity. And the linear approximate model of the planar UM at its equilibrium points is uncontrollable [7,8]. Thus, studying the point-to-point position control approaches of the planar UM is challenging. In addition, the study on the planar underactuated manipulator is more significant for promoting the development of underactuated mechanical system theory.

Usually, the planar UM with a passive joint has the different characteristics [9]. According to the integrability condition in [10], such planar UM is classified into three categories: the first is the holonomic manipulator, which has the angle constraint [11], the second is the first-order nonholonomic manipulator, which has the angular velocity constraint [12], and the third is the second-order nonholonomic manipulator [13].

The holonomic system [14] is controlled based on an angle constraint and the first-order nonholonomic systems [15] are controlled based on an angular velocity constraint. The control methods for these two types of systems are quite mature. However, as for the second-order nonholonomic system, there is no angle or angular velocity constraints available, so such system is more difficult to control than the above two types of systems.

Among the second-order nonholonomic manipulators, the planar Pendubot is a two-link manipulator with second passive joint. For this system, Luca [16] uses the NA method to compute a suitable cycle control input and proposes an iterative steering approach to stabilize the system.

For a planar AAP system having the second-order nonholonomic constraint, Arai [17] proposes a control method to construct trajectories composed of translational and rotational trajectories for positioning the planar AAP system. And Luca [18] presentes a stable control method for a planar A^nP ($n > 2$) system based on the trajectory planning. Meanwhile, the above methods all rely on the center of the percussion of the last link. Such methods can only work for manipulators with the passive link located at the end.

The three-link manipulator with passive first joint (pla-

Manuscript received October 23, 2019; revised February 12, 2020; accepted March 12, 2020. Recommended by Aldo Jonathan Munoz-Vazquez under the direction of Editor Won-jong Kim. This work is supported by the National Natural Science Foundation of China under Grant 61773353, the Hubei Provincial Natural Science Foundation of China under Grant 2015CFA010, and the 111 project under Grant B17040.

Zixin Huang, Xuzhi Lai, Pan Zhang, Yawu Wang, and Min Wu are with the School of Automation, China University of Geosciences, 388 Lumo Road, Hongshan District, Wuhan 430074, China, and also with the Hubei Key Laboratory of Advanced Control and Intelligent Automation for Complex Systems, Wuhan 430074, China (e-mails: {huangzixin, laixz, zhpan, wangyawu, wumin}@cug.edu.cn).
* Corresponding author.

nar PAA system) can be controlled by the angular velocity constraint [15]. The three-link manipulator with passive last joint (planar AAP system) can be controlled by the chained form [17]. However, there is a little researching on a planar UM with a passive middle joint (PMJ), whose simplest form is the planar APA system. [19] pointes the control problem of the planar APA system remains open. In addition, the existing methods of the PAA type and AAP type cannot be suitable for the APA type. Thus, the control method of the planar APA system is not mature, and there is no effective control method for such system.

Nowadays, to study the control problem of the planar UM with a PMJ, we take the planar APA system as the research object, and propose a control method for the system by reducing it to two virtual parts. First, we get the target angle range of the first active link (FAL) relying on the target position of end-point and geometrical relationship. Then, the original system is reduced to a PVP by controlling the passive joint reach to its target position and the states of the third active link (TAL) be zero. Next, we design an open-loop control law for the FAL based on the NA model, which can make the FAL and second underactuated link (SUL) stop rotating and the FAL come back to its target angle. Hence, the original system is further reduced to PVA with the static motion of all links. According to the target value of end-point and the angle constraint of PVA, we calculate the two links' target angles of PVA using PSO algorithm [20]. Then, the controllers are designed to make the TAL reach to its target states and to keep the FAL at its target states. Meanwhile, the SUL is adjusted to its target states based on the angle constraint. Thus, the end-point of the planar APA system can reach to the target position. At last, one simulation example is taken to verify our presented strategy.

2. THE MODEL

The model of the planar APA system is shown in Fig. 1, where ◎ represents the active joints and ◯ represents the passive joint. The parameters of the ith $(i = 1,2,3)$ link are: q_i is the angle, m_i is the mass, L_i is the length, L_{ci} is the distance from its joint to its center of mass, J_i is the moment of inertia, and τ_i is the torque of the ith joint, (x,y) is the end-point coordinate.

The dynamic equations of the system is

$$M(q)\ddot{q} + H(q,\dot{q}) = \tau, \tag{1}$$

where $q = [q_1\ q_2\ q_3]^T$, $\dot{q} = [\dot{q}_1\ \dot{q}_2\ \dot{q}_3]^T$, and $\ddot{q} = [\ddot{q}_1\ \ddot{q}_2\ \ddot{q}_3]^T$ are the vector of angle, angular velocity and angular acceleration, respectively; $\tau = [\tau_1\ 0\ \tau_3]^T$ is the input torque vector; $M(q) \in \mathbb{R}^{3\times3}$ is the inertia matrix with the characteristic of the symmetric positive definite, and $H(q,\dot{q}) \in \mathbb{R}^{3\times1}$ contains the Coriolis and centrifugal forces. For a detailed expression of M and H, see [15].

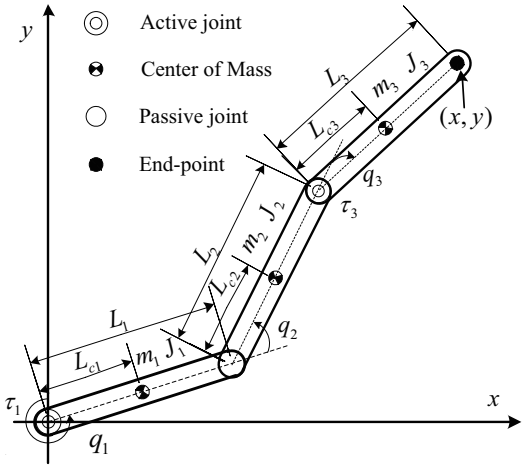

Fig. 1. Planar APA System.

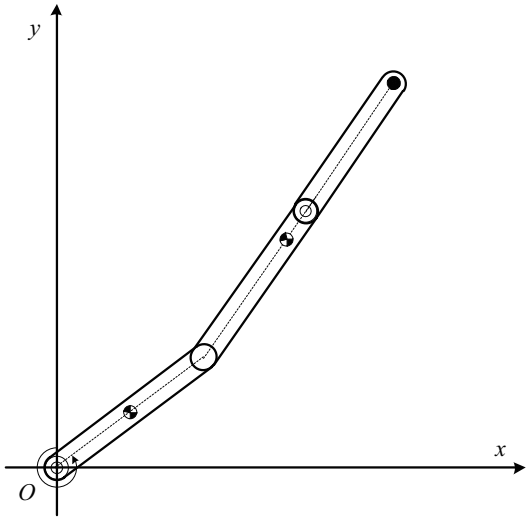

Fig. 2. Sketch of the PVP.

Because the planar APA system has complex nonlinear characteristics, there is no way to achieve its stable control. However, the stable control of planar Pendubot has been realized by employing NA model and that of planar Acrobot has been achieved by using angle constraint.

Motivated by the above stable control strategies of two kinds of two-link systems, we divide the planar APA system into two parts to control by analyzing its mechanical structure. When the angle and the angular velocity of the third link of the planar APA system are controlled to zero, that is, $q_3 = 0$ and $\dot{q}_3 = 0$, the last two links can be regarded as a virtual passive link. In this case, the planar APA system is treated as a PVP. The PVP is shown as Fig. 2, where we mainly implement the control objective of the FAL. When the angle of the first link of the planar APA system is kept at a constant, the planar APA system is treated as a PVA. The PVA is shown as Fig. 3, where we mainly realize the control objectives of the SUL and TAL.

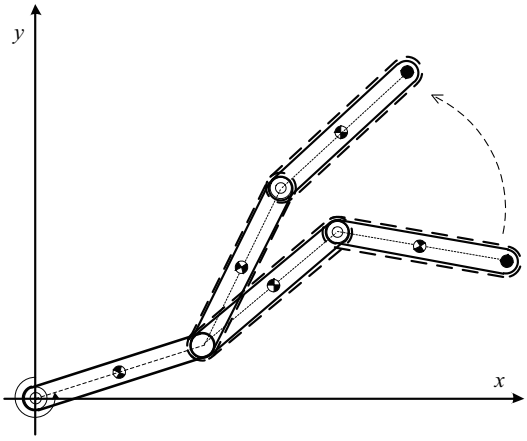

Fig. 3. Sketch of the PVA.

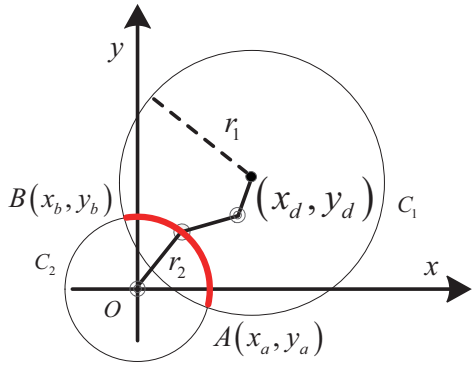

Fig. 4. Sketch of the target area of the passive joint.

3. CONTROLLER DESIGN FOR PVP

We achieve the control objective of FAL for the PVP in this section, and make the system be reduced to a PVA with all links stopping rotating.

3.1. Target angle solution of the FAL

This subsection uses a geometry method to get the FAL's target angle corresponding to the target value of end-point.

For Fig. 4, we firstly draw a circle C_1, where the center of the circle is target position, and radius r_1 is a sum of the length of the SUL and TAL. Then, we draw another circle C_2, where the center of the circle is the inertial coordinate origin, and the radius r_2 is the length of the FAL. The points on the two circles can be described:

$$\begin{cases} C_1 : (x-x_d)^2 + (y-y_d)^2 = r_1^2, \\ C_2 : x^2 + y^2 = r_2^2, \end{cases} \tag{2}$$

where $r_1 = L_2 + L_3$, $r_2 = L_1$, and (x_d, y_d) is target position.

The intersections of above two circles are $A(x_a, y_a)$ and $B(x_b, y_b)$. For the control objective, the controllable region of the passive joint is the red AB arc of Fig. 4. Therefore, when the periodicity of the angle is not taken into consideration, the angle of the FAL at A, B are q_1^A, q_1^B, respectively. Thus, the range of the target angle of FAL, defined as q_1^d, is

$$q_1^d \in \left[q_1^A, q_1^B\right]. \tag{3}$$

3.2. System reduced to PVP

We achieve the control objective of $q_1 = q_1^d$, $\dot{q}_1 = 0$, $q_3 = 0$, and $\dot{q}_3 = 0$ in this subsection. That is, the original system is regarded as PVP.

Let $x = [x_1\ x_2\ x_3\ \ x_4\ x_5\ x_6]^T = [q_1\ q_2\ q_3\ \ \dot{q}_1\ \dot{q}_2\ \dot{q}_3]^T$, and the dynamic model (1) can be transformed to the following state-space equation.

$$\begin{cases} \dot{x}_1 = x_4, \\ \dot{x}_2 = x_5, \\ \dot{x}_3 = x_6, \\ \dot{x}_4 = f_1 + g_{11}\tau_1 + g_{13}\tau_3, \\ \dot{x}_5 = f_2 + g_{21}\tau_1 + g_{23}\tau_3, \\ \dot{x}_6 = f_3 + g_{31}\tau_1 + g_{33}\tau_3, \end{cases} \tag{4}$$

where g_{11}, g_{21}, g_{31}, g_{13}, g_{23}, and g_{33} are nonlinear functions, and f_1, f_2, and f_3 satisfy

$$[f_1\ \ f_2\ \ f_3] = M^{-1}(q)\, H(q, \dot{q}). \tag{5}$$

Equation (4) is further expressed to be

$$\dot{x} = f(x) + g(x)\,\tau, \tag{6}$$

where

$$\begin{cases} f(x) = [x_4, x_5, x_6, f_1, f_2, f_3]^T, \\ g(x) = [g_1, g_2]^T, \end{cases} \tag{7}$$

where g_1 is a 3×3 null matrix and

$$g_2(x) = \begin{bmatrix} g_{11} & 0 & g_{13} \\ g_{21} & 0 & g_{23} \\ g_{31} & 0 & g_{33} \end{bmatrix} = M^{-1} \begin{bmatrix} 1 & 0 & 0 \\ 0 & 0 & 0 \\ 0 & 0 & 1 \end{bmatrix}. \tag{8}$$

The following Lyapunov function is chosen for the control objective of this subsection

$$V_1(x) = \frac{1}{2} P_1 \left(x_1 - x_1^d\right)^2 + \frac{1}{2} x_4^2 + \frac{1}{2} P_2 x_3^2 + \frac{1}{2} x_6^2, \tag{9}$$

where P_1, P_2 are positive constants, and $x_1^d = q_1^d$. The derivative of V_1 is

$$\begin{aligned} \dot{V}_1(x) =& x_4 \left(P_1 \left(x_1 - x_1^d\right) + f_1 + g_{11}\tau_1 + g_{13}\tau_3\right) \\ &+ x_6 \left(P_2 x_3 + f_3 + g_{31}\tau_1 + g_{33}\tau_3\right). \end{aligned} \tag{10}$$

Thus, the controllers are chosen as

$$\begin{cases} \tau_1 = \left(P_1\left(-x_1 + x_1^d\right) - f_1 - D_1 x_4 - g_{13}\tau_3\right) {g_{11}}^{-1}, \\ \tau_3 = \left(P_2\left(-x_3\right) - f_3 - D_2 x_6 - g_{31}\tau_1\right) {g_{33}}^{-1}, \end{cases} \tag{11}$$

where D_1, D_2 are positive constants. From (8), we obtain

$$g_{11} = \frac{M_{22}M_{33} - M_{23}^2}{\det M}, \quad g_{33} = \frac{M_{11}M_{22} - M_{12}^2}{\det M}, \tag{12}$$

which are positive [15].

Substituting (11) into (10) obtains

$$\dot{V}_1(x) = -D_1 x_4^2 - D_2 x_6^2 \le 0. \tag{13}$$

Substituting (11) into (6), the closed loop system (CLS) is

$$\dot{x} = F_p(x). \tag{14}$$

From (13), $V_1(x)$ is bounded. Define

$$\Omega_1 = \left\{x \in \mathbb{R}^6 \,|V_1(x) \le \lambda_1\right\}, \tag{15}$$

where $\lambda_1 > 0$. Next, any solution x of (14) starting in Ω_1 remains in Ω_1 for all $t \ge 0$. Let Φ_1 be an invariant of the CLS (14)

$$\Phi_1 = \left\{x(t) \in \Omega_1 \left|\dot{V}_1(x) = 0\right.\right\}. \tag{16}$$

When $\dot{V}_1(x) \equiv 0$, then $x_4 \equiv 0$ and $x_6 \equiv 0$. Substituting it into (6) gets

$$\begin{cases} f_1 = -g_{11}\tau_1 - g_{13}\tau_3, \\ f_3 = -g_{31}\tau_1 - g_{33}\tau_3. \end{cases} \tag{17}$$

Substituting (17) into (11) obtains $x_1 = x_1^d, x_3 = 0$. Then, the largest invariant set for the FAL and TAL states of the original system in this stage is

$$W_1 = \left\{x \in \mathbb{R}^6 \mid x_1 = q_1^d, x_3 = 0, x_4 = 0, x_6 = 0\right\}. \tag{18}$$

From LaSalle's invariance principle [21], the controllers have completed control objectives of this subsection, which are $q_1 = q_1^d$, $\dot{q}_1 = 0$ and $q_3 = 0$, $\dot{q}_3 = 0$.

Thus, when the following conditions S_{1a} are satisfied, the system is reduced to the PVP.

$$S_{1a} := \begin{cases} \left|x_1 - x_1^d\right| \le e_1, \quad |x_4| \le e_2, \\ |x_3| \le e_1, \quad |x_6| \le e_2, \end{cases} \tag{19}$$

where e_1, e_2 are small positive constants.

Based on (1), the underactuated constraint is

$$M_{21}\ddot{q}_1 + M_{22}\ddot{q}_2 + M_{23}\ddot{q}_3 + H_2 = 0. \tag{20}$$

From [15], we know H_2 is a polynomial about $(\dot{q}_1)^2$ and $\dot{q}_3$. Combining (18) and (20), when we achieve the objective of this subsection, the states of SUL are $\dot{x}_5 \equiv 0$ and $x_5 = \varepsilon$ (ε is a constant). Therefore, the original system is regarded as PVP. Meanwhile, the control objective of the FAL of PVP has been achieved, but the SUL keeps rotating due to the underactuated characteristic.

Note that the initial angular velocities of all links should be zero when we employ the constraints of PVA to realize control objectives of the SUL and TAL. Thus, in the next subsection, we use the NA method to ensure that the SUL stops rotating when the FAL reaches to its target states.

3.3. Stable control for PVP

In this subsection, we design a cycle controller to make the two links of PVP be stationary, and to ensure that the SUL reaches to a middle angle, while states of the FAL at the starting moment of each period are the same as that at the last moment. Meanwhile, the states of TAL are kept being zero during the whole control stage, which ensures that the system is always a PVP.

Fig. 5 shows the model of PVP. Its dynamic model is expressed as

$$\tilde{M}(\tilde{q})\ddot{\tilde{q}} + \tilde{H}\left(\tilde{q}, \dot{\tilde{q}}\right) = \tilde{\tau}, \tag{21}$$

where

$$\tilde{M}(\tilde{q}) = \begin{bmatrix} \tilde{M}_{11} & \tilde{M}_{12} \\ \tilde{M}_{21} & \tilde{M}_{22} \end{bmatrix}, \quad \tilde{H}\left(\tilde{q}, \dot{\tilde{q}}\right) = \begin{bmatrix} \tilde{H}_1\left(\tilde{q}, \dot{\tilde{q}}\right) \\ \tilde{H}_2\left(\tilde{q}, \dot{\tilde{q}}\right) \end{bmatrix}, \tag{22}$$

$$\tilde{q} = \left[\tilde{q}_1 \ \tilde{q}_2\right]^T, \quad \dot{\tilde{q}} = \left[\dot{\tilde{q}}_1 \ \dot{\tilde{q}}_2\right]^T, \quad \tilde{\tau} = \left[\tilde{\tau}_1 \ 0\right]^T, \tag{23}$$

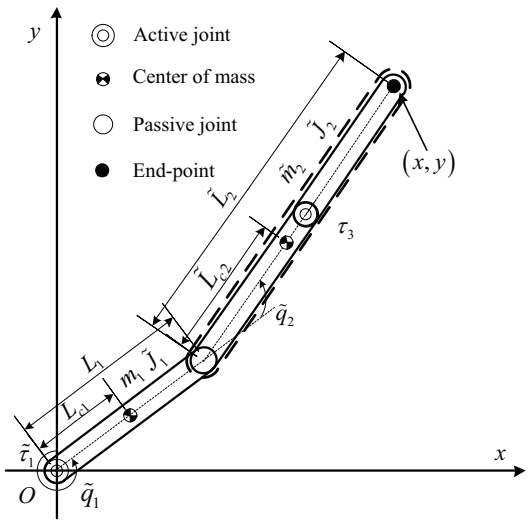

Fig. 5. The model of the PVP.

$$\begin{cases} \tilde{M}_{11} = b_1 + b_2 + 2b_3\cos\tilde{q}_2, \\ \tilde{M}_{12} = \tilde{M}_{21} = b_2 + b_3\cos\tilde{q}_2, \\ \tilde{M}_{22} = b_2, \\ \tilde{H}_1 = -b_3\left(2\dot{\tilde{q}}_1\dot{\tilde{q}}_2 + \left(\dot{\tilde{q}}_2\right)^2\right)\sin\tilde{q}_2, \\ \tilde{H}_2 = b_3\left(\dot{\tilde{q}}_1\right)^2\sin\tilde{q}_2 \end{cases} \tag{24}$$

$$\begin{cases} b_1 = m_1{L_{c1}}^2 + (m_2+m_3){L_1}^2 + \tilde{J}_1, \\ b_2 = (m_2+m_3)\left(L_{c2}+L_{c3}\right)^2 + \tilde{J}_2, \\ b_3 = (m_2+m_3)L_1\left(L_{c2}+L_{c3}\right). \end{cases} \tag{25}$$

The underacutated constraint of (21) is

$$\tilde{M}_{21}\ddot{\tilde{q}}_1 + \tilde{M}_{22}\ddot{\tilde{q}}_2 + \tilde{H}_2 = 0. \tag{26}$$

Define $\ddot{\tilde{q}}_1 = u$, so we get

$$\begin{cases} \ddot{\tilde{q}}_1 = u, \\ \ddot{\tilde{q}}_2 = -\tilde{M}_{22}^{-1}\tilde{H}_2 - \tilde{M}_{22}^{-1}\tilde{M}_{21}u. \end{cases} \tag{27}$$

Combining (21) and (27), we get

$$\tilde{\tau}_1 = \left(\tilde{M}_{11} - \tilde{M}_{12}\tilde{M}_{22}^{-1}\tilde{M}_{21}\right)u + \tilde{H}_1 - \tilde{M}_{12}\tilde{M}_{22}^{-1}\tilde{H}_2. \tag{28}$$

Let $\tilde{x} = [\tilde{q}_1\ \tilde{q}_2\ \dot{\tilde{q}}_1\ \dot{\tilde{q}}_2]^T$, so the state-space equation of PVP is

$$\begin{aligned} \dot{\tilde{x}} &= \begin{bmatrix} \dot{\tilde{q}}_1 \\ \dot{\tilde{q}}_2 \\ 0 \\ -N\sin\tilde{q}_2\left(\dot{\tilde{q}}_1\right)^2 \end{bmatrix} + \begin{bmatrix} 0 \\ 0 \\ 1 \\ -(1+N\cos\tilde{q}_2) \end{bmatrix} u \\ &= \tilde{f}(\tilde{x}) + \tilde{g}(\tilde{x})u, \end{aligned} \tag{29}$$

where $N = b_3/b_2$.

According to the state equation (29), we can adopt the iterative steering approach [22] to make the two links of the PVP stop rorating, and make the states of the FAL be the same at the starting and last moment of each period.

Fig. 6 shows the control sequence diagram for controlling PVP. According to the Fig. 6, we define the period of the iterative steering control as T, the initial time of iterative steering as $\tilde{t}_0 = t_1$ and the initial states $\tilde{x}_0$ of the PVP as

$$\tilde{x}_0 = x(t_1) = \left[\tilde{q}_1^0\ \tilde{q}_2^0\ \dot{\tilde{q}}_1^0\ \dot{\tilde{q}}_2^0\right] = \left[q_1^1\ q_2^1\ 0\ \dot{q}_2^1\right], \tag{30}$$

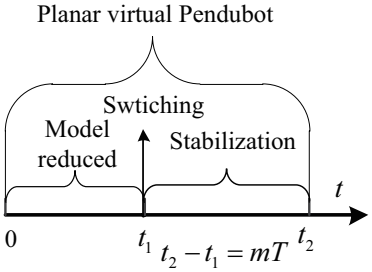

Fig. 6. Control sequence.

where $q_1^1 = q_1^d$.

When the PVP is stable, we define the termination time as $\tilde{t}_m = t_2$ and the final state as $\tilde{x}_m = x(t_2)$.

$$\tilde{x}_m = \left[\tilde{q}_1^m\ \tilde{q}_2^m\ 0\ 0\right] = \left[q_1^d\ q_2^m\ 0\ 0\right]. \tag{31}$$

Based on the above definition, we give the procedure of the iterative steering:

Step 1: Set $\tilde{t}_0 = t_1$, $t_2 - t_1 = mT$, $\tilde{t}_k = \tilde{t}_0 + kT$ and $k = 1, \cdots, m$. Define $\tilde{x}_k$ as the state at the kth period. $\tilde{x}_k$ needs to be closer to $\tilde{x}_m$ than $\tilde{x}_{k-1}$.

Step 2: Control the PVP to the state $\tilde{x}_k$, and k starts from 1 to m.

Step 3: Iterative the open-loop control input $u(\tilde{x}_{k+1})$ from $u(\tilde{x}_k)$ that controls the state from $\tilde{x}_k$ to $\tilde{x}_{k+1}$ in $[\tilde{t}_k, \tilde{t}_{k+1}]$. In general, the $\tilde{x}_k \neq \tilde{x}_m$.

Step 4: Set $\tilde{t}_{k+1} = \tilde{t}_k + T$. If $\tilde{x}_{k+1} = \tilde{x}_m$, the iterative steering is finished. Otherwise, go to **Step 2**.

During the iterative steering, the states of the system at the end of each cycle should be

$$\begin{cases} \tilde{q}_1^k = \tilde{q}_1(\tilde{t}_k) = q_1^d, \\ \dot{\tilde{q}}_1^k = \dot{\tilde{q}}_1(\tilde{t}_k) = 0, \\ \tilde{q}_2^k = \tilde{q}_2(\tilde{t}_k), \\ \dot{\tilde{q}}_2^k = \dot{\tilde{q}}_2(\tilde{t}_k). \end{cases} \tag{32}$$

After m iteration periods of control, the controller ensures that the SUL stops rotating. At the same time, the SUL converges to its middle angle $\tilde{q}_2^m$.

$$\begin{cases} \tilde{q}_2^{k=m} = \tilde{q}_2(\tilde{t}_m) = \tilde{q}_2^m, \\ \dot{\tilde{q}}_2^{k=m} = \dot{\tilde{q}}_2(\tilde{t}_m) = 0. \end{cases} \tag{33}$$

For achieving the control objectives, we employ the NA model to calculate the cyclic control input in the iterative steering approach.

Luca [16] has studied the algorithm for NA model of the underactuated system. Thus, we reference the proposed method to compute the NA model for the PVP (29). Similarly, we construct the accessible matrix by choosing the vector fields $\{\tilde{f}, \tilde{g}, [\tilde{f}, \tilde{g}], [\tilde{g}, [\tilde{f}, \tilde{g}]]\}$ to make coordinate transformation and get the privileged coordinates at $[\tilde{q}_1^0\ \tilde{q}_2^0\ \dot{\tilde{q}}_1^0\ \dot{\tilde{q}}_2^0]$ of the PVP as follows:

$$\begin{cases} \tilde{q}_1 = \tilde{q}_1^0 - z_3, & \text{(34a)} \\ \tilde{q}_2 = \tilde{q}_2^0 + \dot{\tilde{q}}_2^0 z_1 + \alpha z_3, & \text{(34b)} \\ \dot{\tilde{q}}_1 = z_2, & \text{(34c)} \\ \dot{\tilde{q}}_2 = \dot{\tilde{q}}_2^0 - \alpha z_2 + \beta z_3 - \gamma z_4 + \beta z_1 z_2, & \text{(34d)} \end{cases}$$

where $\alpha = 1 + N\cos\tilde{q}_2^0$, $\beta = N\dot{\tilde{q}}_2^0\sin\tilde{q}_2^0$, $\gamma = N^2\sin 2\tilde{q}_2^0$.

The NA model of the PVP is

$$\begin{cases} \dot{z}_1 = 1, & \text{(35a)} \\ \dot{z}_2 = u, & \text{(35b)} \\ \dot{z}_3 = -z_2, & \text{(35c)} \\ \dot{z}_4 = \dfrac{z_2^2}{2N\cos\tilde{q}_2^0} - \left(\dfrac{\left(\dot{\tilde{q}}_2^0\right)^2 z_1^2}{4N\sin\tilde{q}_2^0} + \dfrac{\alpha z_3}{2N\cos\tilde{q}_2^0}\right)u & \text{(35d)} \end{cases}$$

Thus, we use the NA model (35) instead of the exact model (29) for computing the control input.

Since the system goes through a cycle of control, the states of the FAL should return to $\left(q_1^d, 0\right)$. Thus, according to $\ddot{\tilde{q}}_1 = u$, u should satisfy the conditions

$$\int_0^T u(t)\mathrm{d}t = 0, \quad \int_0^T \int_0^t u(\tau)\mathrm{d}\tau\mathrm{d}t = 0. \tag{36}$$

From (35b), (35c) and (36), we find that

$$\begin{cases} z_2(T) = \int_0^T u(t)\mathrm{d}t = 0, & \text{(37a)} \\ z_3(T) = -\int_0^T \int_0^t u(\tau)\,\mathrm{d}\tau\mathrm{d}t = 0. & \text{(37b)} \end{cases}$$

According to (34b) and (37b), we obtain the angle error of SUL at $k = 1$ period.

$$\Delta\tilde{q}_2 = \tilde{q}_2^1 - \tilde{q}_2^0 = \dot{\tilde{q}}_2^0 z_1(T) = \dot{\tilde{q}}_2^0 T. \tag{38}$$

Since $z_1(t) = \int_0^T \dot{z}_1\mathrm{d}t = T$ from (35a), (38) indicates $\Delta\tilde{q}_2$ does not depend on the control input, but only depends on $\dot{\tilde{q}}_2^0$.

According to (34d) and (37), we can obtain the angular velocity error of SUL at $k = 1$ period.

$$\Delta\dot{\tilde{q}}_2 = \dot{\tilde{q}}_2^1 - \dot{\tilde{q}}_2^0 = -\gamma z_4(T). \tag{39}$$

From (35d), we get

$$\begin{aligned} z_4(T) = &\int_0^T \frac{1}{2N\cos\tilde{q}_2^0} z_2^2(t)\mathrm{d}t \\ &-\int_0^T \left(\frac{\left(\dot{\tilde{q}}_2^0\right)^2}{4N\sin\tilde{q}_2^0} z_1^2(t) + \frac{\alpha}{2N\cos\tilde{q}_2^0} z_3(t) \right) u(t)\mathrm{d}t. \end{aligned} \tag{40}$$

Based on partial integration method, the relative items of (40) can be obtained

$$\begin{cases} \int_0^T z_1^2(t)u(t)\mathrm{d}t = \int_0^T z_1^2(t)\mathrm{d}z_2(t) \\ \qquad = (z_1^2(t)z_2(t))|_0^T - 2\int_0^T z_1(t)\dot{z}_1(t)z_2(t)\mathrm{d}t \\ \qquad = -2\int_0^T z_1(t)z_2(t)\mathrm{d}t \\ \qquad = 2\int_0^T z_1(t)\mathrm{d}z_3(t) \\ \qquad = 2\left(z_1(t)z_3(t)\right)|_0^T - 2\int_0^T \dot{z}_1(t)z_3(t)\mathrm{d}t \\ \qquad = -2\int_0^T z_3(t)\mathrm{d}t, \\ \int_0^T z_3(t)u(t)\mathrm{d}t = \int_0^T z_3(t)\mathrm{d}z_2(t) \\ \qquad = (z_3(t)z_2(t))|_0^T - 2\int_0^T \dot{z}_3(t)z_2(t)\mathrm{d}t \\ \qquad = \int_0^T z_2^2(t)\mathrm{d}t. \end{cases} \tag{41}$$

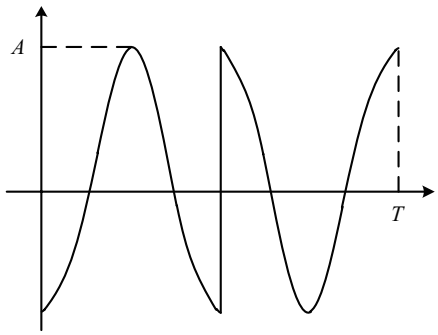

Fig. 7. Profile of u.

From (39), (40) and (41), we can obtain

$$\begin{aligned} \Delta\dot{\tilde{q}}_2 = &N^2\sin\tilde{q}_2^0\cos\tilde{q}_2^0\int_0^T z_2^2(t)\mathrm{d}t \\ &-N\cos\tilde{q}_2^0\left(\dot{\tilde{q}}_2^0\right)^2\int_0^T z_3(t)\mathrm{d}t, \end{aligned} \tag{42}$$

where the sign of the two items on the right depends only on $\tilde{q}_2^0$ and $\left(\dot{\tilde{q}}_2^0\right)^2$, respectively.

The cyclic control input $u(t)$ is designed as

$$u(t) = \begin{cases} -A\cos\dfrac{4\pi t}{T}, & t \in \left[0, \dfrac{T}{2}\right), \\ A\cos\dfrac{4\pi\left(t - \frac{T}{2}\right)}{T}, & t \in \left[\dfrac{T}{2}, T\right]. \end{cases} \tag{43}$$

where the A (see Fig. 7) is the amplitude of $u(t)$.

From (35b) and (35c), $\ddot{z}_3 = -u$ is obtained. Thus,

$$\int_0^T z_3(t)\mathrm{d}t = \int_0^T \int_0^t \int_0^\sigma u(\rho)\,\mathrm{d}\rho\mathrm{d}\sigma\mathrm{d}t = 0, \tag{44}$$

and

$$\int_0^T z_2^2(t)\mathrm{d}t = \int_0^T \left(\int_0^t u(\sigma)\,\mathrm{d}\sigma\right)^2 \mathrm{d}t = \frac{T^3}{32\pi^2}A^2. \tag{45}$$

According to (42), (44) and (45),

$$\Delta\dot{\tilde{q}}_2 = \frac{A^2T^3N^2}{64\pi^2}\sin 2\tilde{q}_2^0. \tag{46}$$

The above expression indicates $\Delta\dot{\tilde{q}}_2$ and $\sin 2\tilde{q}_2^0$ have the same sign.

To ensure that the states of the SUL are closer to the given values by the iterative steering after every period, we give the contracting relationship of the first period as follows:

$$\left|\tilde{q}_2^m - \tilde{q}_2^1\right| \le \eta_1\left|\tilde{q}_2^m - \tilde{q}_2^0\right|, \tag{47}$$

$$\left|\dot{\tilde{q}}_2^1\right| \le \eta_2\left|\dot{\tilde{q}}_2^0\right|. \tag{48}$$

where η_1, $\eta_2 \in [0, 1)$ are coefficients of convergence.

Without loss of generality, assume

$$\tilde{q}_2^m - \tilde{q}_2^1 = \eta_1 \left(\tilde{q}_2^m - \tilde{q}_2^0\right), \tag{49}$$

$$\dot{\tilde{q}}_2^1 = \eta_2 \dot{\tilde{q}}_2^0. \tag{50}$$

Observing (38) and (49), we get

$$T = (1-\eta_1)\frac{\tilde{q}_2^m - \tilde{q}_2^0}{\dot{\tilde{q}}_2^0}, \ \ 0 \le \eta_1 < 1. \tag{51}$$

Because $T > 0$, the following conditions should be satisfied when (51) holds.

$$\begin{cases} \tilde{q}_2^0 < \tilde{q}_2^m, \\ \dot{\tilde{q}}_2^0 > 0, \end{cases} \text{ or } \begin{cases} \tilde{q}_2^0 > \tilde{q}_2^m, \\ \dot{\tilde{q}}_2^0 < 0. \end{cases} \tag{52}$$

And according to (39), (46) and (50), we obtain

$$A = \frac{8\pi}{NT}\sqrt{\frac{\dot{\tilde{q}}_2^0(\eta_2 - 1)}{T\sin 2\tilde{q}_2^0}}, \ \ 0 \le \eta_2 < 1. \tag{53}$$

In order to guarantee the square root in above equation to be positive, the following conditions should be obeyed:

$$\dot{\tilde{q}}_2^0 < 0: \begin{cases} \tilde{q}_2^0 \in Q_1, \\ \tilde{q}_2^0 \in Q_3, \end{cases} \quad \dot{\tilde{q}}_2^0 > 0: \begin{cases} \tilde{q}_2^0 \in Q_2, \\ \tilde{q}_2^0 \in Q_4, \end{cases} \tag{54}$$

where Q_1, Q_2, Q_3 and Q_4 are four quadrants.

Combining (52) and (54), we obtain the following four conditions, where as long as one condition is satisfied, the convergence of the PVP can be realized by using (51) and (53).

$$\begin{cases} \tilde{q}_2^m \in Q_1, \ \tilde{q}_2^0 \in Q_1, \ \tilde{q}_2^0 > \tilde{q}_2^m, \ \dot{\tilde{q}}_2^0 < 0, & \text{(55a)} \\ \tilde{q}_2^m \in Q_2, \ \tilde{q}_2^0 \in Q_2, \ \tilde{q}_2^0 < \tilde{q}_2^m, \ \dot{\tilde{q}}_2^0 > 0, & \text{(55b)} \\ \tilde{q}_2^m \in Q_3, \ \tilde{q}_2^0 \in Q_3, \ \tilde{q}_2^0 > \tilde{q}_2^m, \ \dot{\tilde{q}}_2^0 < 0, & \text{(55c)} \\ \tilde{q}_2^m \in Q_4, \ \tilde{q}_2^0 \in Q_4, \ \tilde{q}_2^0 < \tilde{q}_2^m, \ \dot{\tilde{q}}_2^0 > 0. & \text{(55d)} \end{cases}$$

Here, we define S_{1b}: = (55a) or (55b) or (55c) or(55d). Then, only when S_{1b} is satisfied, we can continue to do iterate steering and realize the stable control of PVP by employing controllers (28).

In order to guarantee the system is reduced to PVP and realize the stable control of PVP, the controllers should be switched from (11) to (28) when the switch condition S_1: $= S_{1a} \cup S_{1b}$ is satisfied.

When the following switch condition S_2 is satisfied,

$$S_2 := \begin{cases} |q_1 - q_1^d| \le e_1, \ \ |\dot{q}_1| \le e_2, \\ |q_2 - \tilde{q}_2^m| \le e_1, \ \ |\dot{q}_2| \le e_2, \\ |q_3| \le e_1, \ \ |\dot{q}_3| \le e_2, \end{cases} \tag{56}$$

the stable control of the PVP is realized using the controller (28).

So far, the target angle of the FAL has been achieved and the planar APA system has been stabilized with all links' angular velocities being zero, which means the planar APA system is reduced to the PVA.

4. CONTROLLER DESIGN FOR PVA

In this section, we realize the control objective of PVA. That is, we control the TAL to its target value, also bringing the SUL to its.

4.1. Modeling for PVA

Fig. 8 shows a model of PVA. Because the initial value of this stage is the termination value of the previous stage, at this stage, we let the initial states of the PVA be $\left[\theta_p^0 \ \ q_3^0 \ \ 0 \ \ 0\right]$, where $q_3^0 = 0$. The θ_p^0 is also expressed as

$$\begin{cases} \theta_p^0 = q_1^d + q_2^m, \\ q_2^m = \tilde{q}_2^m. \end{cases} \tag{57}$$

The dynamic equation of PVA is

$$\hat{M}(\hat{q})\ddot{\hat{q}} + \hat{H}\left(\hat{q}, \dot{\hat{q}}\right) = \hat{\tau}, \tag{58}$$

where

$$\hat{M}(\hat{q}) = \begin{bmatrix} \hat{M}_{22} & \hat{M}_{23} \\ \hat{M}_{32} & \hat{M}_{33} \end{bmatrix}, \ \ \hat{H}\left(\hat{q}, \dot{\hat{q}}\right) = \begin{bmatrix} \hat{H}_1\left(\hat{q}, \dot{\hat{q}}\right) \\ \hat{H}_2\left(\hat{q}, \dot{\hat{q}}\right) \end{bmatrix}, \tag{59}$$

$$\hat{q} = [\theta_p \ \ q_3]^T, \ \ \hat{\tau} = [0 \ \ \hat{\tau}_3]^T, \tag{60}$$

$$\begin{cases} \hat{M}_{22} = c_1 + c_2 + 2c_3\cos q_3, \\ \hat{M}_{23} = \hat{M}_{32} = c_2 + c_3\cos q_3, \\ \hat{M}_{33} = c_2, \\ \hat{H}_1 = -c_3\left(2\dot{\theta}_p\dot{q}_3 + (\dot{q}_3)^2\right)\sin q_3, \\ \hat{H}_2 = c_3\left(\dot{\theta}_p\right)^2\sin q_3, \end{cases} \tag{61}$$

$$\begin{cases} c_1 = m_2{L_{c2}}^2 + m_3{L_2}^2 + \hat{J}_1, \\ c_2 = m_3{L_{c3}}^2 + \hat{J}_2, \\ c_3 = m_3 L_2 L_{c3}. \end{cases} \tag{62}$$

The passive part of (58) is

$$\hat{M}_{22}\ddot{\theta}_p + \hat{M}_{23}\ddot{q}_3 + \hat{H}_1 = 0. \tag{63}$$

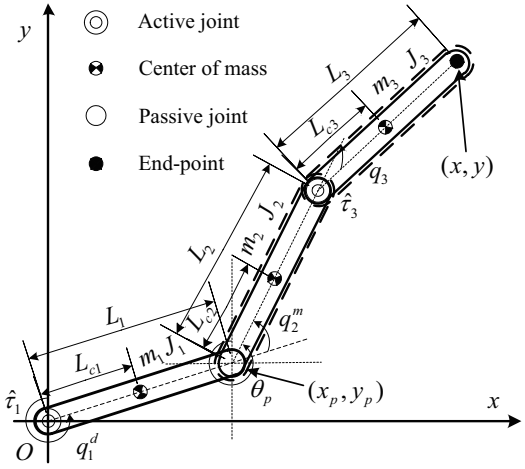

Fig. 8. The model of the PVA.

The PVA is a holonomic system. Thus, integrating (63) can get the following angular velocity constraint [11] when all links are motionless at initial time.

$$\hat{M}_{22}\dot{\theta}_p + \hat{M}_{23}\dot{q}_3 = 0. \tag{64}$$

When $\dot{q}_3 = 0$, $\dot{\theta}_p = 0$. Then, integrating (64), we obtain the angle constraint of PVA [11].

$$\theta_p = -\frac{q_3}{2} - \delta\left(\varphi\tan\frac{q_3}{2} - \varphi\tan\frac{q_3^0}{2} + j\pi\right) + \xi, \quad j \in \mathbb{Z}, \tag{65}$$

where

$$\begin{cases} \delta = \dfrac{c_2 - c_1}{\sqrt{(c_1+c_2)^2 - 4c_3^2}}, \quad \xi = \theta_p^0 + \dfrac{q_3^0}{2}, \\ \varphi = \arctan(\phi\psi), \quad \phi = \sqrt{\dfrac{c_1+c_2-2c_3}{c_1+c_2+2c_3}}, \\ \psi = \tan\left(\dfrac{q_3}{2}\right). \end{cases} \tag{66}$$

From (65), when the TAL reaches to a given angle, the SUL is simultaneously brought to a given angle. In other words, when the TAL is controlled to its target states, the PVA is stabilized at the target position.

4.2. Solution of target angles

In this subsection, the target angles of two links of PVA are solved according to the following constraint relationships by using PSO algorithm: (i) the geometric constraint relationship between the angles of all links; (ii) the reachable area of the FAL, which is selected as a suitable value; (iii) the states of the SUL satisfying S_{1b}; (iv) the angle constraint of the PVA, which is given by (65).

From Fig. 8, we get

$$\begin{cases} x = -\sin q_1^d L_1 - \sin\theta_p L_2 - \sin(\theta_p + q_3) L_3, \\ y = \cos q_1^d L_1 + \cos\theta_p L_2 + \cos(\theta_p + q_3) L_3. \end{cases} \tag{67}$$

According to (3), we can obtain the reachable area of the FAL. The angle of the FAL is adjusted to q_1^d, which can guarantee the end-point reaches to its target position.

Considering the above constraint relationships, the PSO algorithm is introduced to calculate the middle angle of SUL q_2^m and the target angle of the TAL q_3^d.

The iterative rule is as follows:

$$\begin{cases} s_k^\delta(t+1) = s_k^\delta(t) + v_k^\delta(t+1), \\ v_k^\delta(t+1) = \omega v_k^\delta(t) + w_1\mu_1\left(g_k^\delta - s_k^\delta(t)\right) \\ \qquad\qquad + w_2\mu_2\left(b^\delta - s_k^\delta(t)\right), \end{cases} \tag{68}$$

where $\delta = 1, 2, \cdots, S$; $k = 1, 2, \cdots, N$; t is the distance traveled by each particle; s_k^δ and v_k^δ are the location and velocity of the kth particle, respectively; g_k^δ and b^δ are the best location and global best location, respectively; ω is the inertia weight; μ_1, $\mu_2 \in [0,1]$; w_1 and w_2 are the weighting factors.

The following evaluation function is defined for the PSO algorithm

$$h = |x - x_d| + |y - y_d|, \tag{69}$$

where (x,y) is calculated from (67). Let $s_k = \left(s_k^1, s_k^2\right)$ be a 2-dimensional vector, in which s_k^1 and s_k^2 stand for $\tilde{q}_2^m$ and q_3^d, respectively. The procedure flow of the PSO algorithm is as follows:

Step 1: Initialize the particle location s_k^δ, and the particle velocity v_k^δ.

Step 2: Use the angle constraint (65) and a suitable target angle of first link q_1^d to calculate $\tilde{q}_2^m$ in the stage of the stable control of the PVP and q_3 in the stage of the stable control for the PVA. Calculate $h(\cdot)$ for s_k^δ and v_k^δ respectively. If the value of $h(\cdot)$ for s_k^δ is less than the value of $h(\cdot)$ for g_k^δ, then set $g_k^\delta = s_k^\delta$.

Step 3: Calculate $h(\cdot)$ for b^δ. If there is a g_k^δ for which the value of $h(\cdot)$ is less than the value of $h(\cdot)$ for b^δ, then set $b^\delta = g_k^\delta$.

Step 4: If the value of $h(\cdot) \le e_3$ for b^δ, stop. Otherwise, use (68) to update all the locations and velocities, and jump to **Step 2**.

We calculate the coordinates of end-point by using the values of q_1^d, θ_p, and q_3 generated by the PSO algorithm. Also, calculate the value of (69) using those angles. If the result is less than the constant e_3, then the middle angle of the SUL is q_2^m and target angles of the SUL and TAL are q_2^d, q_3^d.

4.3. Controller design for PVA

In this subsection, we realize the control objective of PVA. That is, we maintain the FAL at the target states, and we control the TAL to its target states, which also brings the SUL to its target states.

The following Lyapunov function is chosen based on the control objective of this stage

$$V_2(x) = \frac{1}{2}P_1(x_1 - x_1^d)^2 + \frac{1}{2}x_4^2 + \frac{1}{2}P_2(x_3 - x_3^d)^2 + \frac{1}{2}x_6^2, \tag{70}$$

where P_1, P_2 are positive constants, $x_1^d = q_1^d$ and $x_3^d = q_3^d$. The derivative of V_2 is

$$\begin{aligned} \dot{V}_2(x) =& x_4(P_1(x_1 - x_1^d) + f_1 + g_{11}\tau_1 + g_{13}\tau_3) \\ &+ x_6(P_2(x_3 - x_3^d) + f_3 + g_{31}\tau_1 + g_{33}\tau_3). \end{aligned} \tag{71}$$

So the controllers are designed as

$$\begin{cases} \tau_1 = \left(P_1\left(-x_1 + x_1^d\right) - f_1 - D_1 x_4 - g_{13}\tau_3\right) {g_{11}}^{-1}, \\ \tau_3 = \left(P_2\left(-x_3 + x_3^d\right) - f_3 - D_2 x_6 - g_{31}\tau_1\right) {g_{33}}^{-1}. \end{cases} \tag{72}$$

The CLS of this stage is

$$\dot{x} = F_a(x). \tag{73}$$

Similar to the first stage control of the PVP, we define

$$\begin{cases} \Omega_2 = \left\{ x \in \mathbb{R}^6 \,|\, V_2(x) \le \lambda_2 \right\}, \\ \Phi_2 = \left\{ x(t) \in \Omega_2 \,\middle|\, \dot{V}_2(x) = 0 \right\}, \end{cases} \tag{74}$$

where $\lambda_2 > 0$. The largest invariant set in this stage is

$$W_2 = \left\{ x \in \mathbb{R}^6 | x_i = q_i^d,\ x_{i+3} = 0 \right\},\ \ (i = 1,2,3). \tag{75}$$

From LaSalle′s invariance principle, the controllers have completed control objectives of this subsection, which are $q_1 = q_1^d$, $\dot{q}_1 = 0$, $q_2 = q_2^d$, $\dot{q}_2 = 0$ and $q_3 = q_3^d$, $\dot{q}_3 = 0$.

Under the above control, the controllers (72) force all links to be stabilized at the target angles, which means the control objective of the original system is fulfilled.

5. SIMULATIONS

The simulations are implemented based on Matlab tool for verifying the proposed control strategy. Table 1 shows the parameters of the planar APA system.

The parameters in the switch conditions (19) and (56) are $e_1 = 0.001$ rad, and $e_2 = 0.001$ rad/s.

Remark 1: In the switch conditions (19) and (56), the small positive numbers e_1 and e_2 mean that the states of the system are close to the given states. Through extensive simulation experiments, we choose small positive number to be within a small range with 0.001 as center.

Therefore, $e_3 = 0.001$ m. The parameters of the controllers (11) and (72) are $P_1 = 1$, $P_2 = 1$, $D_1 = 1.8$, and $D_2 = 1.8$.

The amplitude A of $u(t)$ is calculated by (53). T is chosen as a constant at the stable control for PVP. However, it is impossible to choose arbitrarily the angle iteration contraction rate η_1 of the SUL, which only depends on $\tilde{q}_2^0$ from (38). According to (38) and (50), when we use small enough T, η_2 is

$$\eta_2 = \frac{\tilde{q}_2^m - \tilde{q}_2^0 - T\dot{\tilde{q}}_2^0}{\tilde{q}_2^m - \tilde{q}_2^0} = 1 + \frac{\dot{\tilde{q}}_2^0}{\tilde{q}_2^0 - \tilde{q}_2^m} T < 1. \tag{76}$$

We choose $[q_{10}, q_{20}, q_{30}, \dot{q}_{10}, \dot{q}_{20}, \dot{q}_{30}]$ and (x_d, y_d) as

$$\begin{cases} [q_{10}, q_{20}, q_{30}, \dot{q}_{10}, \dot{q}_{20}, \dot{q}_{30}]^{\mathrm{T}} = [-1, 0.5, 0, 0, 0, 0]^{\mathrm{T}}, \\ (x_d, y_d) = (0.2, 0.8)\ \text{m}. \end{cases} \tag{77}$$

Table 1. Model parameters of the planar APA system.

Link i	m_i (kg)	L_i (m)	l_i (m)	J_i (kg·m^2)
$i = 1$	0.7	0.7	0.35	0.0286
$i = 2$	0.6	0.6	0.30	0.0180
$i = 3$	0.5	0.5	0.25	0.0104

According to the reachable area constraint (3), we can obtain the reachable area of the FAL $q_1^d \in [-1.8504, 1.3605]$rad and choose $q_1^d = -1.8000$ rad.

Form (68), the parameters for the PSO algorithm are chosen as $w_1 = 2$, $w_2 = 2$, $\omega = 0.9$, $N = 24$ and $S = 2$. At the same time, since the target angles of all links corresponding to one target position of end-point are multi-solution and periodic, we randomly initialize the positions of first and second particles within range of $\pi/2$ to π and -2π to 2π, respectively. Therefore, employing the PSO algorithm to calculate the middle angle of SUL and the target angles of SUL and TAL gets

$$[q_2^m, q_2^d, q_3^d]^{\mathrm{T}} = [2.8757, 2.4670, 5.8390]^{\mathrm{T}} \text{ rad}. \tag{78}$$

Fig. 9 shows that: firstly, the FAL is stabilized at its target angle, the TAL is controlled to zero and the SUL is

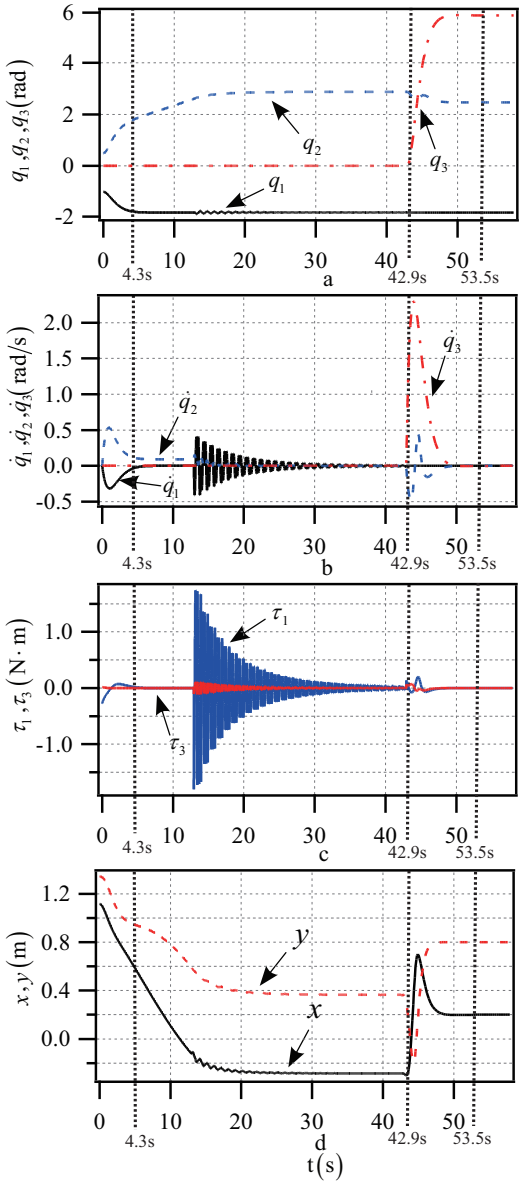

Fig. 9. Simulation results.

rotating at a constant speed at $t = 4.3$ s. Thus, the control objective of this stage is fulfilled and the original system is regarded as PVP.

Then, the states of TAL are kept in zero so that the system is always a PVP from $t = 4.3$ s to $t = 42.9$ s. The SUL is stabilized at its middle angle $q_2^m = 2.8757$ rad at $t = 42.9$ s. That is the control in this stage is fulfilled and the original system is regarded as PVA.

Next, the angle of the FAL is maintained at its target value, which ensures the passive joint is always in its target position and the system is a PVA. Finally, at $t = 53.5$ s, the TAL is stabilized at its target angle $q_3^d = 5.8390$ rad, while bringing the SUL to its target angle $q_2^d = 2.4670$ rad. At the same time, the end-point reaches to $(0.2000, 0.8002)$ m, which means the position control objective of the planar APA system is achieved.

6. CONCLUSION

Our paper develops a position control approach for the planar APA system. For realizing the control objective, the control is divided into two parts based on the NA model of PVP and the complete integrability of PVA. First, the designed controllers make the states of the TAL be zero and the FAL be stabilized at its target angle, that means the system is reduced to a PVP. Then, the NA method is applied to design a stabilization controller for the PVP to realize its stable control. In the stage of PVA, the target angles are calculated by the PSO algorithm according to the holonomic characteristic of PVA. Then, the controllers make the FAL and TAL move to their target values, and the SUL is brought to its target value according to the angle constraint of PVA. Simulation results demonstrate its validity.

What is worth mentioning is the main advantage of this paper is that a novel control method is proposed for the three-link underactuated manipulator with the passive middle joint. Moreover, our control method can enrich the control method of underactuated system and promote the development of the control theory of underactuated system.

REFERENCES

[1] N. T. Binh, N. A. Tung, D. P. Nam, and N. H. Quang, "An adaptive backstepping trajectory tracking control of a tractor trailer wheeled mobile robot," *International Journal of Control, Automation and Systems*, vol. 17, no. 2, pp. 465-473, January 2019.

[2] M. Elfeky, M. Elshafei, A. A. Saif, and M. F. Al-Malki, "Modeling and simulation of quadrotor UAV with tilting rotors," *International Journal of Control, Automation and Systems*, vol. 14, no. 4, pp. 1046-1054, June 2016.

[3] H. Chen and N. Sun, "Nonlinear control of underactuated systems subject to both actuated and unactuated state constraints with experimental verification," *IEEE Trans. on Industrial Electronics*, 2019. DOI: 10.1109/TIE.2019.2946541

[4] N. Sun, Y. Fu, T. Yang, J. Y. Zhang, Y. C. Fang, and X. Xin, "Nonlinear motion control of complicated dual rotary crane systems without velocity feedback: Design, analysis, and hardware experiments," *IEEE Trans. on Automation Science and Engineering*, vol. 17, no. 2, pp. 1017-1029, 2020.

[5] D. Liu, X. Z. Lai, Y. W. Wang, X. B. Wan, and M. Wu, "Position control for planar four-link underactuated manipulator with a passive third joint," *ISA Transactions*, vol. 87, pp. 46-54, April 2019.

[6] P. Zhang, X. Z. Lai, Y. W. Wan, and M. Wu, "Motion planning and adaptive neural sliding mode tracking control for positioning of uncertain planar underactuated manipulator," *Neurocomputing*, vol. 334, pp. 197-205, January 2019.

[7] J. D. Wu, Y. W. Wang, W. J. Ye, and C. Y. Su, "Control strategy based on Fourier transformation and intelligent optimization for planar Pendubot," *Information Sciences*, vol. 491, pp. 279-288, July 2019.

[8] P. Zhang, X. Z. Lai, Y. W. Wan, C. Y. Su, W. J. Ye, and M. Wu, "A novel position-posture control method using intelligent optimization for planar underactuated mechanical systems," *Mechanism and Machine Theory*, vol. 140, pp. 258-273, June 2019.

[9] Y. Liu and H. Yu, "A survey of underactuated mechanical systems," *IET Control Theory Applications*, vol. 7, no. 7, pp. 921-935, July 2013.

[10] G. Oriolo and Y. Nakamur, "Control of mechanical systems with second-order nonholonomic constraints: underactuated manipulators," in *Proceedings of the IEEE International Conference on Decision and Control*, Brighton, England, pp. 2398-2403, 1991.

[11] X. Z. Lai, J. H. She, W. H. Cao, and S. X. Yang, "Stabilization of underactuated planar acrobot based on motion-state constraints," *International Journal Non-Linear Mechanics*, vol. 77, pp. 342-347, December 2015.

[12] Y. Sheng, X. Z. Lai, and M. Wu, "Position control of a planar three-link underactuated mechanical system based on model reduction," *Acta Automatica Sinica*, vol. 40, no. 7, pp. 1303-1310, July 2014.

[13] T. Zilic, J. Kasac, Z. Situm, and M. Essert, "Simultaneous stabilization and trajectory tracking of underactuated mechanical systems with included actuators dynamics," *Multibody System Dynamics*, vol. 29, no. 1, pp. 1-19, January 2013.

[14] J. Q. Cao, X. Z. Lai, and M. Wu, "Position control method for a planar Acrobot based on fuzzy control," *Proceedings of the Chinese Control Conference*, Hangzhou, China, pp. 923-927, 2015.

[15] X. Z. Lai, Y. W. Wang, M. Wu, and W. H. Cao, "Stable control strategy for planar three-link underactuated mechanical system," *IEEE/ASME Trans. on Mechatronics*, vol. 21, no. 3, pp. 1345-1356, January 2016.

[16] A. D. Luca, R. Mattone, and G. Oriolo, "Stabilization of an underactuated planar 2R manipulator," *International Journal of Robust and Nonlinear Control*, vol. 10, no. 4, pp. 181-198, March 2000.

[17] H. Arai, K. Tanie, and N. Shiroma, "Nonholonomic control of a three-DOF planar underactuated manipulator," *IEEE Trans. on Robotics and Automation*, vol. 14, no. 5, pp. 681-695, October 1998.

[18] A. D. Luca and G. Oriolo, "Trajectory planning and control for planar robots with passive last joint," *International Journal Robotics Research*, vol. 21, no. 5-6, pp. 575-590, May-June 2002.

[19] A. D. Luca, S. Iannitti, R. Mattone, and G. Oriolo, "Underactuated manipulators: control properties and techniques," *Machine Intelligence and Robotic Control*, vol. 4, no. 3, pp. 113-126, May 2003.

[20] H. Wang, H. Sun, C. H. Li, S. Rahnamayan, and J. S. Pan, "Diversity enhanced particle swarm optimization with neighborhood search," *Information Sciences*, vol. 223, pp. 119-135, February 2013.

[21] J. P. LaSalle, "Stability theory for ordinary differential equations," *Journal of Differential Equations*, vol. 4, no. 1, pp. 57-65, January 1968.

[22] P. Lucibello and G. Oriolo, "Stabilization via iterative state steering with application to chained-form systems," *Proceedings of the IEEE International Conference on Decision and Control*, Kobe, Japan, pp.2614-2619, 1996.

Zixin Huang received his B.S. and M.S. degrees in engineering from Wuhan Textile University, Wuhan, China, in 2013 and 2016, respectively. He is currently pursuing a Ph.D. degree at the School of Automation, China University of Geosciences, Wuhan, China. His current research interests include robot control, nonlinear system control, and intelligent control.

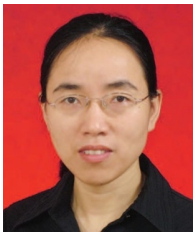

Xuzhi Lai received her B.S., M.S., and Ph.D. degrees in engineering from Central South University, Changsha, China, in 1988, 1991, and 2001, respectively. From 1991 to 2014, she was a Faculty Member of the School of Information Science and Engineering, Central South University, as a Full Professor in 2004. From 1998 to 1999, she was a Visiting Scholar with the Department of Mechatronics, School of Engineering, Tokyo University of Technology, Tokyo, Japan. From 2004 to 2006, she was a Visiting Scholar with the Department of Mechanical and Engineering, University of Toronto, Toronto, ON, Canada, and with the School of Engineering, University of Guelph, Guelph, ON, Canada. In 2014, she moved to the China University of Geosciences, Wuhan, China, where she is currently a Professor with the School of Automation. Her current research interests include intelligent control, robot control, and nonlinear system control.

Pan Zhang received her B.S. degree in engineering from China University of Geosciences, Wuhan, China, in 2015, where she is currently pursuing a Ph.D. degree in control science and engineering with the School of Automation. Since October 2018, she has been a Research Intern with the Department of Mechanical, Industrial and Aerospace Engineering, Concordia University, Montreal, QC, Canada. Her current research interests include nonlinear system control and intelligent control.

Yawu Wang received his B.S. and M.S. degrees in engineering from Hubei University of Technology, Wuhan, China, in 2012 and 2015, respectively. He received his Ph.D. degree in engineering from China University of Geosciences, Wuhan, China, in 2018. He is currently an Associate Professor in the School of Automation, China University of Geosciences, Wuhan, China. His main research interest is robot control and intelligent control.

Min Wu received his B.S. and M.S. degrees in engineering from Central South University, Changsha, China, in 1983 and 1986, respectively, and a Ph.D. degree in engineering from the Tokyo Institute of Technology, Tokyo, Japan, in 1999. He was a Faculty Member at the School of Information Science and Engineering, Central South University, from 1986 to 2014, and became a Professor in 1994. In 2014, he joined the China University of Geosciences, Wuhan, China, where he is currently a Professor at the School of Automation. He was a Visiting Scholar with the Department of Electrical Engineering, Tohoku University, Sendai, Japan, from 1989 to 1990, and a Visiting Research Scholar with the Department of Control and Systems Engineering, Tokyo Institute of Technology, from 1996 to 1999. He was a Visiting Professor at the School of Mechanical, Materials, Manufacturing Engineering and Management, University of Nottingham, Nottingham, U.K., from 2001 to 2002. His current research interests include process control, robust control, and intelligent systems. Dr. Wu is a Fellow of IEEE and a Fellow of the Chinese Association of Automation. He was a corecipient of the International Federation of Automatic Control Control Engineering Practice Prize Paper Award in 1999 (together with M. Nakano and J. She).